

Multiple Pharmacophore Models Combined with Molecular Docking: A Reliable Way for Efficiently Identifying Novel PDE4 Inhibitors with High Structural Diversity

Zhi Chen,^{†,§} Guanghui Tian,^{†,§} Zhen Wang,[†] Hualiang Jiang,^{†,‡} Jingshan Shen,^{*,†} and Weiliang Zhu^{*,†,‡}

Shanghai Institute of Materia Medica, Chinese Academy of Sciences, 555 Zuchongzhi Road, Shanghai 201203, People's Republic of China, and School of Pharmacy, East China University of Science and Technology, Shanghai 200237, People's Republic of China

Received October 29, 2009

Multiple pharmacophore models were constructed based on the 18 crystal structures of phosphodiesterase 4 (PDE4) in complex with different inhibitors for discovering new potential PDE4 inhibitors. After validation of their efficiency in screening, 10 of the pharmacophore models were confirmed effective. Remarkably, the hits retrieved by these effective pharmacophore models were different, demonstrating that different pharmacophore models may have different performances in database screening. Therefore, all these models were employed to screen the compound database SPECS for finding potent leads with much structural diversity. Combining all the screened hits based on the 10 pharmacophore models, followed by molecular docking and bioassay, 4 of 53 tested compounds were found as active as rolipram (a well studied PDE4 inhibitor). More impressively, the four potent inhibitors with different chemical scaffolds were discovered by three different pharmacophore models separately, suggesting that a single pharmacophore model-based screening might not be efficient in thoroughly identifying potential hits from a compound database. This study also revealed that ligand–receptor complex structure-based pharmacophore is more efficient for identifying potent hits with great structural diversity in comparison with ligand-based pharmacophore and similarity search approaches. Therefore, multiple pharmacophore model-based virtual screenings should be used, if available, in combination with molecular docking for fully discovering hit compounds from compound databases.

INTRODUCTION

In the past decade, virtual screening has become a promising tool for discovering drug leads.¹ It is established as one of the most important computational techniques used to separate wanted from unwanted molecules within compound libraries, which has to be done as early as possible in order to reduce drug discovery costs. If the three-dimensional (3D) structure of a target protein is known, the molecular docking method was usually employed. However, when the structure of the target is unavailable, the pharmacophore method was an alternative choice. The pharmacophore model is an interpretation of the interaction between a receptor and a ligand and is clearly established as one of the successful computational tools in rational drug design.^{2,3} Typically, the pharmacophore models are used when some active compounds have been identified, but the 3D structure of the target protein or receptor is unknown. The active compounds are superimposed to determine their common features and, hence, to provide a pharmacophore model that explains ligand–receptor binding. Recently, pharmacophore models could also be derived directly from complex crystal structures, which is the structure-based pharmacophore method.^{4,5} Thanks to

the advantage in efficiency in the virtual screening,^{2,6} the pharmacophore model method is now a potent tool in the area of drug discovery.

LigandScout⁵ is a software tool that allows to rapidly and transparently derive 3D chemical feature-based pharmacophores from structural data of macromolecule–ligand complexes. Its algorithms perform a stepwise interpretation of the ligand molecules: planar ring detection, assignment of functional group patterns, determination of the hybridization state, and finally the assignment of Kekulé pattern.⁷ However, the pharmacophore model derived from one complex structure only reflected limited information on the binding mode of actives. Different pharmacophore models generated from different crystal structures may reflect different inhibitor binding modes, thus, a question is raised that whether each pharmacophore model has a similar performance or capability in identifying potential hits from a compound database. The answer to the question may help to make a decision on how a virtual screening should be carried out if multiple models are available. To the best of our knowledge, no report on the performance of multiple pharmacophore model-based database searching has been reported to date. In this study, the method of multiple pharmacophore models was tested on its efficiency in the discovery of the inhibitors of PDE4.⁸

Cyclic nucleotides are intracellular second messengers that play key roles in many physiological processes. The levels of these nucleotides are tightly regulated at the point of synthesis by receptor-linked enzymes (such as adenylyl or

* Corresponding author's fax: +86-21-50807088 (J.S.) and +86-21-50807088 (W.Z.); e-mail: jsshen@mail.shcnc.ac.cn (J.S.) and wlzhu@mail.shcnc.ac.cn (W.Z.).

[†] Chinese Academy of Sciences.

[‡] East China University of Science and Technology.

[§] These authors contributed equally to this work.

guanylyl cyclase) and at the point of degradation by a family of enzymes known as phosphodiesterases (PDEs).⁹ Consequently, the PDE enzyme family influences a vast array of pharmacological processes, including proinflammatory mediator production and action, ion channel function, muscle contraction, learning, differentiation, apoptosis, lipogenesis, glycogenolysis, and gluconeogenesis. Therefore, PDEs have become recognized as important drug targets for a range of biological disorders, such as retinal degeneration, congestive heart failure, depression, asthma, erectile dysfunction, and inflammation.^{10,11} One of these identified PDE families is PDE4, a cAMP-specific enzyme.⁸ PDE4 is expressed in a number of cell types that is considered suitable drug target for the treatment of respiratory diseases, such as asthma and chronic obstructive pulmonary disease (COPD).¹² There are now over 20 potent inhibitors reported targeting PDE4. However, the developed inhibitors for PDE4, such as rolipram, cilomilast, and roflumilast, displayed common side effects, such as diarrhea, headache, and nausea.^{8,13,14} The other side effects, such as abdominal pain and vomiting, were also reported.¹⁵ Thus it is clear that further improvement for such inhibitors is required. Therefore, it is meaningful to develop novel inhibitors with fewer side effects.

In recent years, more and more crystal structures of PDE4 in complex with small ligands have been reported, providing much information about the structural features of PDE4 inhibitors. Based on the structural information, it is convenient now to carry out structure-based drug design for discovering novel PDE4 inhibitors. Until now, no pharmacophore-based screening has been reported for discovering PDE4 inhibitors.^{16–18} In this study, multiple pharmacophore models were constructed for the same target protein. There are a total of 22 pharmacophore models constructed from the PDE4–inhibitor complex structures. After validation, 10 of 22 pharmacophore models were confirmed effective. Thereafter, the pharmacophore-based screenings were performed with multiple models against the compound database SPECS by using Catalyst on the platform of Discovery Studio (version 2.0, Accelrys Inc., San Diego, CA),² followed by molecular docking with software GOLD^{19–21} and Glide^{22,23} for further cross-validation. Finally, 60 compounds were selected, and 53 compounds were obtained for bioassay, 6 of which are in vitro inhibitors. Four inhibitors with novel structures are as active as a well-recognized PDE4 inhibitor, rolipram. Very impressively, we found that the four novel inhibitors were identified by three different pharmacophore models, respectively, demonstrating that a single pharmacophore-based screening is not an efficient approach for identifying active compounds from a chemical database. Therefore, multiple pharmacophore models should be used simultaneously, if available, for virtual screening in order to fully identify potential hit compounds from a chemical database.

METHODS

Pharmacophore Model Generation. By using software LigandScout^{5,24} with default parameters, 22 initial pharmacophore models were constructed based on 18 complex structures of PDE4 obtained from the Protein Data Bank,²⁴ including 8 PDE4B complex structures (PDB code: 1XM6,

1RO6, 1XLZ, 1XLX, 1XMU, 1XM4, 1Y2J, and 1Y2H; the root-mean-square deviations (rmsd) of each pair of structures are less than 0.6 Å) and 10 PDE4D complex structures (PDB code: 1Y2C, 2FM5, 2FM0, 1XOM, 1XON, 1XOQ, 1TBB, 1Y2E, 1XOR, and 1Y2K; the rmsds of each pair of structures are less than 0.5 Å). The excluded volumes were included for establishing more restrictive and selective pharmacophore models.^{25–27}

Database Preparation and Multiple Pharmacophore Model-Based Screening. For validating the reliability of the 22 constructed pharmacophore models, a decoy database was constructed, as shown in Figure 1A, by mixing the 15 ligands extracted from the complex structures discussed above, from 51 PDE4 inhibitors under clinical development collected from the latest literature,²⁹ and from 10 000 of the most structurally diverse chemicals selected from the database DUD²⁸ with Discovery Studio (DS hereinafter, version 2.0, Accelrys Inc., San Diego, CA). The chemical database SPECS with over 190 000 compounds in 2D SD form were transferred into multiconformer with DS. During the process of database generation, the FAST method was selected, and the maximum number of conformers generated was set to 250. Then, the pharmacophore models were employed one by one with the fast flexible search method to screen the databases with DS. The number of hits was limited with the maxhits option to 200 000.

Molecular Docking. GOLD was first used to screen all the compounds identified by the multiple pharmacophore model-based screening. The crystal structures of 1RO6³⁰ (PDE4B) and 2FM0³¹ (PDE4D) were employed for docking as they have the highest resolution and relatively intact structures. The active sites were defined to encompass any protein atom within 10 Å radius sphere centered on the mass of the cocrystallized ligands in the complex structures, and a 7–8 times speedup setting was selected in virtual screening. All the other variable parameters had the default values. The compounds in MOL2 format were flexibly docked into the binding site of the targets, respectively. The literature result demonstrated that the GoldScore function displayed similar or superior results than those of ChemScore in selecting compounds,²¹ so we selected the GoldScore function to rank the compounds.

Glide^{22,23} was used for further cross-validation. Target protein protonation was treated with the pprep script in Glide. Glide constructed a grid that defined the ligand-binding site search region, which was centered on the cocrystallized ligand in the complex structure. The grid was defined as an enclosing box with 15 Å in all three dimensions. The standard precision (SP) docking mode was selected. The ligands in the MOL2 format were transformed into MAE format with mol2convert utility encoded in the program and then docked flexibly into the binding site.

Isolation of PDE4s. PDE4s were purified by anion exchange chromatography from rat kidneys by a modification of a previously described method.³² All procedures were carried out at 0–4 °C. Briefly, fresh tissue was minced and homogenized in 5 volumes of HEPES buffer [20 mM of HEPES, 0.25 M of sucrose, 1 mM of EDTA, 1 mM of phenylmethyl sulfonyl fluoride (PMSF), pH of 7.2]. The homogenate was centrifuged at 100 000 g for 60 min at 4 °C. The supernatant was filtered through a 0.2 µm pore filter. PDE4s in the soluble fractions were separated using a

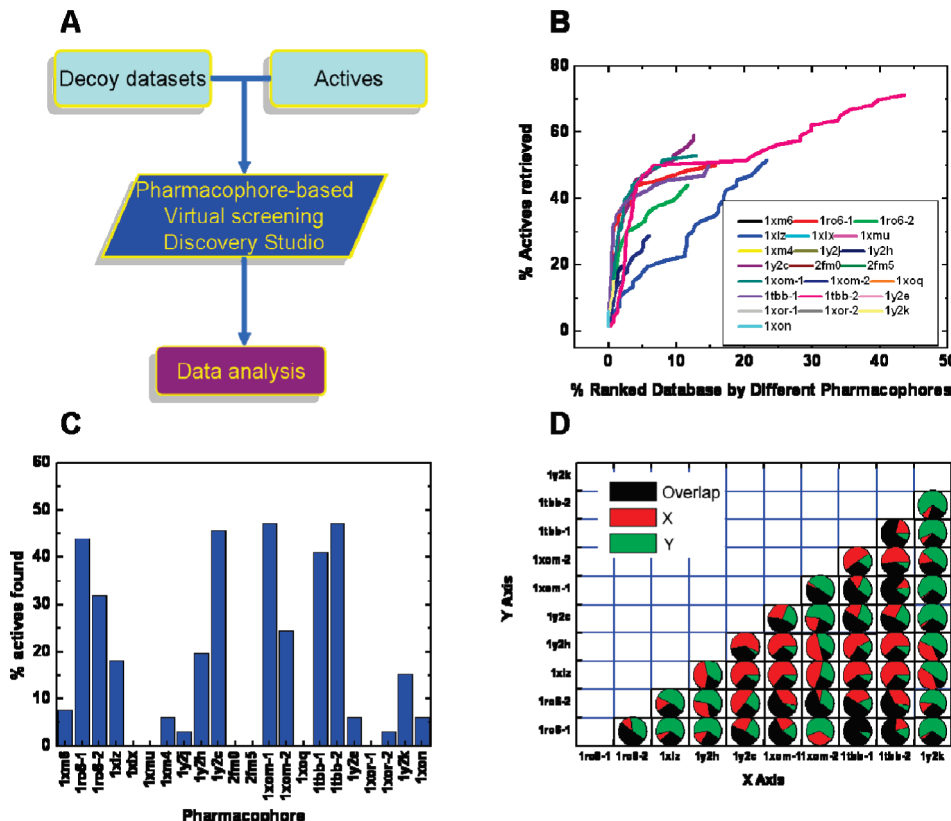


Figure 1. (A) The flowchart of the validation process for the constructed pharmacophore models. (B) The recovery rate of the known actives from the constructed decoy database versus the ranked database screened with different pharmacophore models. The codes with -1 and -2 are the two pharmacophore models generated from the two different conformations of the same ligand in the crystal structure. (C) The total recovery rate of the known actives in the top 5% of the rank database screened by different pharmacophore models. (D) The alignment of the known actives recovered by the two corresponding pharmacophore models. The parts colored red and green represent the numbers of the hit compounds, while the part colored black is the overlap section of the screened hit compounds.

Pharmacia FPLC system (Pharmacia Ltd., Milton Keynes, U.K.) with a Mono Q anion exchange column (8 mL bed volume, Pharmacia Ltd.). The Mono Q column was pre-equilibrated with 20 mM HEPES buffer (pH of 7.2), containing 2 mM of EDTA, 1 mM of benzamide, and 1 mM of PMSF, followed by an application of a 20 mL sample of tissue soluble fraction. PDE4s were eluted using a linear gradient of sodium chloride (0–1M) in the same buffer (pH of 7.2) at a flow rate of 1.5 mL/min, and 3 mL fractions were collected over a 90 min period. PDE4 activities in each fraction were determined, and then fractions containing PDE4 activities were pooled.

PDE4 Assays. Compounds were evaluated for inhibitory activity against PDE4 in two steps. The first step was the determination of the percentage of inhibition at 50 μ M performed in duplicate with rolipram as control, which is a well studied PDE4 inhibitor. For the compounds displaying a percentage of inhibition greater than that of rolipram, the IC₅₀ was determined from a concentration-response curve using concentrations of 10 and 100 nM and 1, 10, and 100 μ M. PDE4s activity was analyzed using a tritium scintillation proximity assay (SPA) system, and the assay was performed according to the manufacturer's instructions (Amersham Biosciences). Briefly, assays were performed in the presence of 50 mM of Tris-HCl (pH of 7.5), containing 8.3 mM of MgCl₂ and 1.7 mM of EGTA. Each assay was performed in a 100 μ L reaction volume containing the above buffer, PDE4s and around 0.05 μ Ci [³H]cAMP. The reaction was carried out at 30 °C for 30 min and stopped by the addition

of 50 μ L of PDE SPA beads (1 mg) suspended in 18 mM of zinc sulfate. The reaction mixture was left to be settled at room temperature for 20 min before counting in a MicroBeta TriLux (Perkin-Elmer Life Sciences, USA). PDE4s inhibitory activity was calculated from equation below:

$$\% \text{PDE4s inhibition} = \left[1 - \frac{(\text{CPM}_{\text{sample}} - \text{CPM}_{\text{blank}})}{\text{CPM}_{\text{control}} - \text{CPM}_{\text{blank}}} \right] \times 100$$

In this equation, CPM_{sample} represents the radioactive value of the sample obtained from the assay (with enzyme); CPM_{control} represents the radioactive value of the solvent (water) which was used for diluting the sample obtained from the assay (with enzyme); CPM_{blank} represents the radioactive value of the mixture of only buffer and substrate (without enzyme). IC₅₀ values were calculated from the concentration-inhibition curves by nonlinear regression analysis using GraphPad Prism.

RESULTS

Construction of Pharmacophore Models for PDE4. Twenty-two pharmacophore models were generated from 18 crystal structures of the protein-ligand complexes (refer to Supporting Information for details). As an example, one pharmacophore model generated from 1XM6³³ for PDE4B was displayed in Figure 2A. The water molecules in the crystal structure, which do not mediate hydrogen bonds

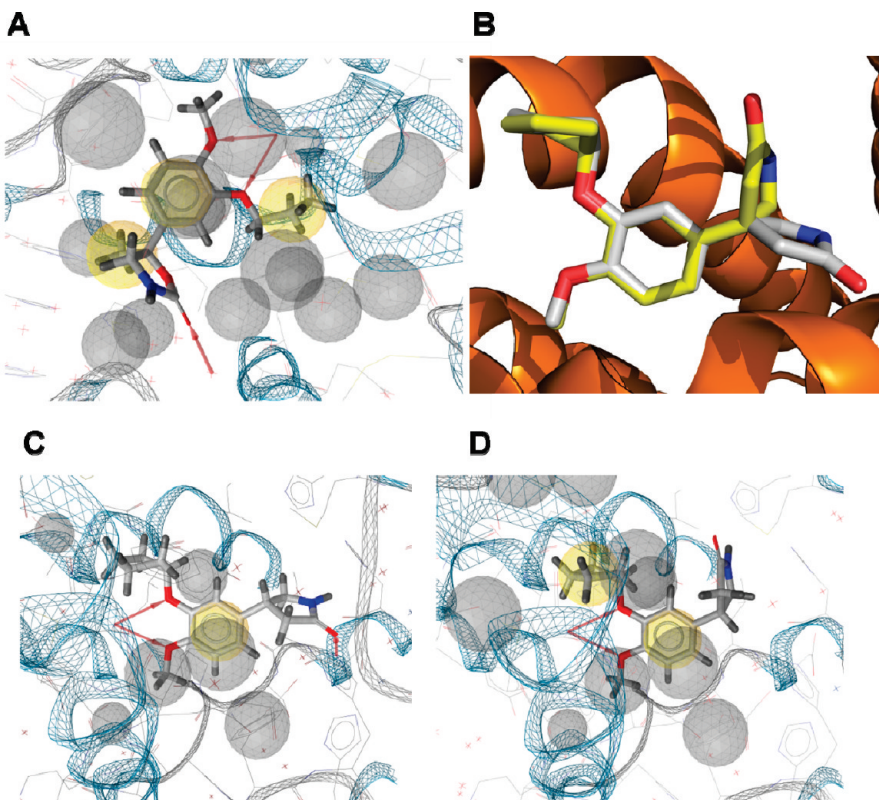


Figure 2. (A) The pharmacophore model generated from crystal structure of 1XM6 by LigandScout. The red arrow represents the hydrogen-bond acceptor, the yellow sphere stands for the hydrophobic group, and the gray sphere represents the excluded volume. (B) The cocrystallized ligand in the crystal structure of 1RO6. The ligands colored white and yellow represent two different binding conformations of the same ligand, accordingly; two pharmacophore models (C, D) were generated.

between the ligand and the receptor, were deleted. After modification, the final pharmacophore model consists of 3 hydrophobic groups, 3 hydrogen-bond acceptors, and 15 excluded volumes. Some crystal structures showed different binding conformations of a specific ligand. For instance, in the crystal structure of 1RO6, the ligand displayed two conformations (Figure 2B). Then these two conformations were used to generate two pharmacophore models, respectively, which are different from each other (Figure 2C and D), demonstrating that the same ligand in different binding conformations may have different pharmacophore features.

Validation of the Constructed Pharmacophore Models.

Figure 1B is the recovery rate of the actives against the ranked decoy database screened by the corresponding pharmacophore model, while Figure 1C is the total recovery rate at the top 5% of the ranked database for each pharmacophore model. The results demonstrated that the pharmacophore models generated from 1RO6-1, 1RO6-2, 1XLZ, 1Y2H, 1Y2C, 1XOM-1, 1XOM-2, 1TBB-1, 1TBB-2, and 1Y2K can identify the actives, with a recovery rate of the known actives higher than 15% in the top 5% of the ranked decoy database. Figure 1D is the alignment of the known actives retrieved by different pharmacophore models. The black-colored area represents the overlap section of the recovered actives by the two corresponding pharmacophore models. Therefore, the larger the black-colored area, the more similar the two corresponding pharmacophore models. Only 15 among 45 pairs have the black area larger than 50% of the actives retrieved from each compared pharmacophore pairs, reflecting that the 10 pharmacophore models are quite different from each other. Especially, the pharmacophore models of 1XOM-2 and 1RO6-1 are retrieved completely different

Table 1. The Screening Results by Different Complex Structure-Based Pharmacophore Models

pharmacophore model	hits retrieved
1RO6-1	10 411
1RO6-2	9526
1TBB-1	9525
1TBB-2	23 247
1XLZ	11 594
1XOM-1	12 253
1XOM-2	8975
1Y2C	10 466
1Y2H	1026
1Y2K	375

actives, demonstrating completely different binding features. Hence, multiple pharmacophore models should be employed for thoroughly identifying potential hits. Therefore, the 10 pharmacophore models were all subjected to the virtual screening.

Application of Multiple Pharmacophore Models in Virtual Screening. A fit value is a measure of how well the ligand fits the pharmacophore. Therefore, the hits with a high fit value are probably very active. In this study, the hits retrieved by the pharmacophore models with fit values above 2.0 were regarded as potential hits and remained for further analysis.

The amounts of the hit compounds predicted by each of the 10 pharmacophore models from SPECS are summarized in Table 1. Noticeably, some pharmacophore models were found very restrictive and retrieved very limited hits from SPECS. For example, the pharmacophore model of 1Y2K retrieved only 375 hits. In contrast, 5 pharmacophore models

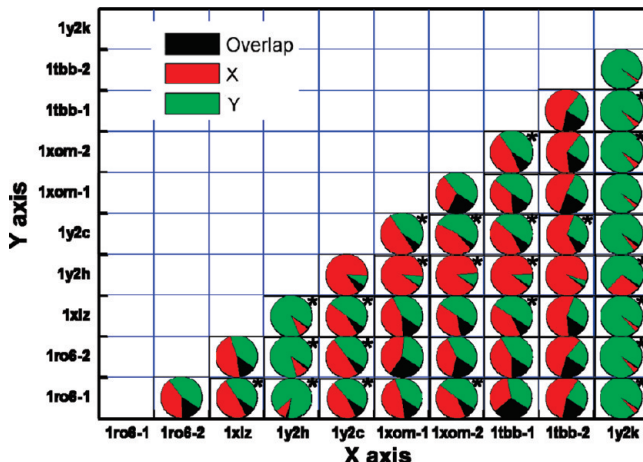


Figure 3. The screening results from the 10 different pharmacophore models. The parts colored red and green represent the numbers of the hits from the two comparing pharmacophore models (Table 1), respectively, and the part colored black represents the overlap section of the screened hit by the two models. The graph with an asterisk represents the case of the overlap section that is less than 30% of the hit number by either pharmacophore model.

(1RO6-1, 1XLZ, 1Y2C, 1XOM-1, and 1TBB-2) identified hits of more than 10 000, demonstrating that different pharmacophore models may have quite different performance in screening a chemical database.

For further analyzing the performance of different pharmacophore models, the overlap section of the hits retrieved from each pair of two different pharmacophore models was analyzed (Figure 3). Impressively, there are 23 pairs in which the overlap section of the hit amounts retrieved from two different pharmacophore models is less than 30%, while the other 22 pairs are higher than 30% (marked with asterisk in Figure 3), but there are no pairs with a overlap area higher than 50%. This result further implied that different pharmacophore models from different crystal structures are different in terms of screening efficiency. Therefore, multiple pharmacophore models should be used to improve the overall screening efficacy and success rate.

After the pharmacophore screening, all the 42 671 hits identified by the multiple pharmacophore models (Table 1) were subjected to molecular docking with GOLD and Glide. Top 10% of the compounds from the GOLD scored hit list were subjected to another docking by Glide. In the ranked list by Glide, 60 compounds with high structural diversity were selected, and 53 of them were obtained for enzymatic activity assay.

The biological test for the 53 samples discovered 6 compounds with an inhibition rate higher than rolipram, a well-known drug as a PDE4 inhibitor. Then the IC₅₀ values of these compounds were determined and revealed that four of the six compounds are potent inhibitors with IC₅₀ values less than 10 μM (Figure 4A and B). Overall, 7.5% of the tested compounds are as active as the positive control rolipram, demonstrating that the multiple pharmacophore model-based database screening in combination with molecular docking is a highly efficient way for discovering active compounds.

All the four inhibitors are significantly different from rolipram and from each other in chemical scaffold (Figure 4B and C). More impressively, they were identified by three different pharmacophore models. As shown in Figure 5A,

the inhibitor **1** was identified by the pharmacophore model of 1XOM-1 with three hydrogen-bond acceptors and one hydrophobic group, with a high fit value of 3.8. In this compound, the cyano group functions as a hydrogen-bond acceptor and the benzene group acts as a hydrophobic group. The inhibitor **2** was identified by the pharmacophore 1RO6-1, revealing a very similar binding mode between the cocrystallized ligand (Figure 5D) and **2** (Figure 5E), i.e., two hydrophobic and two hydrogen-bond receptor features. The binding mode is also similar to the rolipram, validating the rationality of the prediction by the pharmacophore model. The inhibitor **3** was retrieved from the pharmacophore 1XOM-1 as well (Figure 5C). The carboxyl group acts as two hydrogen-bond acceptors, and a nitrogen atom is a hydrogen-bond acceptor. The inhibitor **4** could map onto the pharmacophore 1Y2C (Figure 5F and G) with a fit value of 3.7, demonstrating three hydrophobic groups and one hydrogen-bond acceptor. Impressively, the pharmacophore model of 1TBB retrieved many hits (9525 with 1TBB-1 and 23 247 with 1TBB-2), but none of the four inhibitors were identified by the hypothesis. We also noticed that the pharmacophore model 1RO6 with a high-success rate contains more information than that from 1TBB, demonstrating that the pharmacophore model with less information is weak in identifying a good hit compound.

DISCUSSION

Good-Binding Conformation Predicted by Pharmacophore Model. Four new inhibitors were found targeting PDE4 by employing a multiple pharmacophore model-based screening integrated with docking and bioassay approaches. We found that the four inhibitors could match three different pharmacophore models. However, the binding mode predicted by the pharmacophore model might be different from that predicted by the docking algorithm. To explore the difference, conformation comparison by the two different approaches was carried out.

The rmsd between the pharmacophore predicted conformation and the X-ray determined bioactive conformation of the ligand were calculated, as shown in Table 2. Among 18 tested cases, the pharmacophore method yields 17 cases with rmsd values less than 2.0 Å, however, both GOLD and Glide were found to have only 10 cases with rmsd values less than 2.0 Å, respectively. The average rmsd value by pharmacophore method is 0.83 Å, much less than that by GOLD and Glide (1.93 and 2.21 Å, respectively), demonstrating that the pharmacophore method is better in reproducing the bioactive conformation of the ligand in the binding pocket than either GOLD or Glide.

Figure 6A shows the case that the pharmacophore model failed in reproducing the experimental conformation in the structure 1TBB. LigandScout figured out four features that are important for the binding of the ligand in 1TBB, which are one hydrophobic group on both the cyclopentyl group and the benzene and two hydrogen-bond acceptors on two oxygen atoms (Figure 6A). The pyrrolidinone group of the ligand was not regarded as an important group for the binding. Consequently, the conformation of the group predicted by the pharmacophore model is significantly different from the PDB structure (the green square part in Figure 6A). This result demonstrated that more pharmaco-

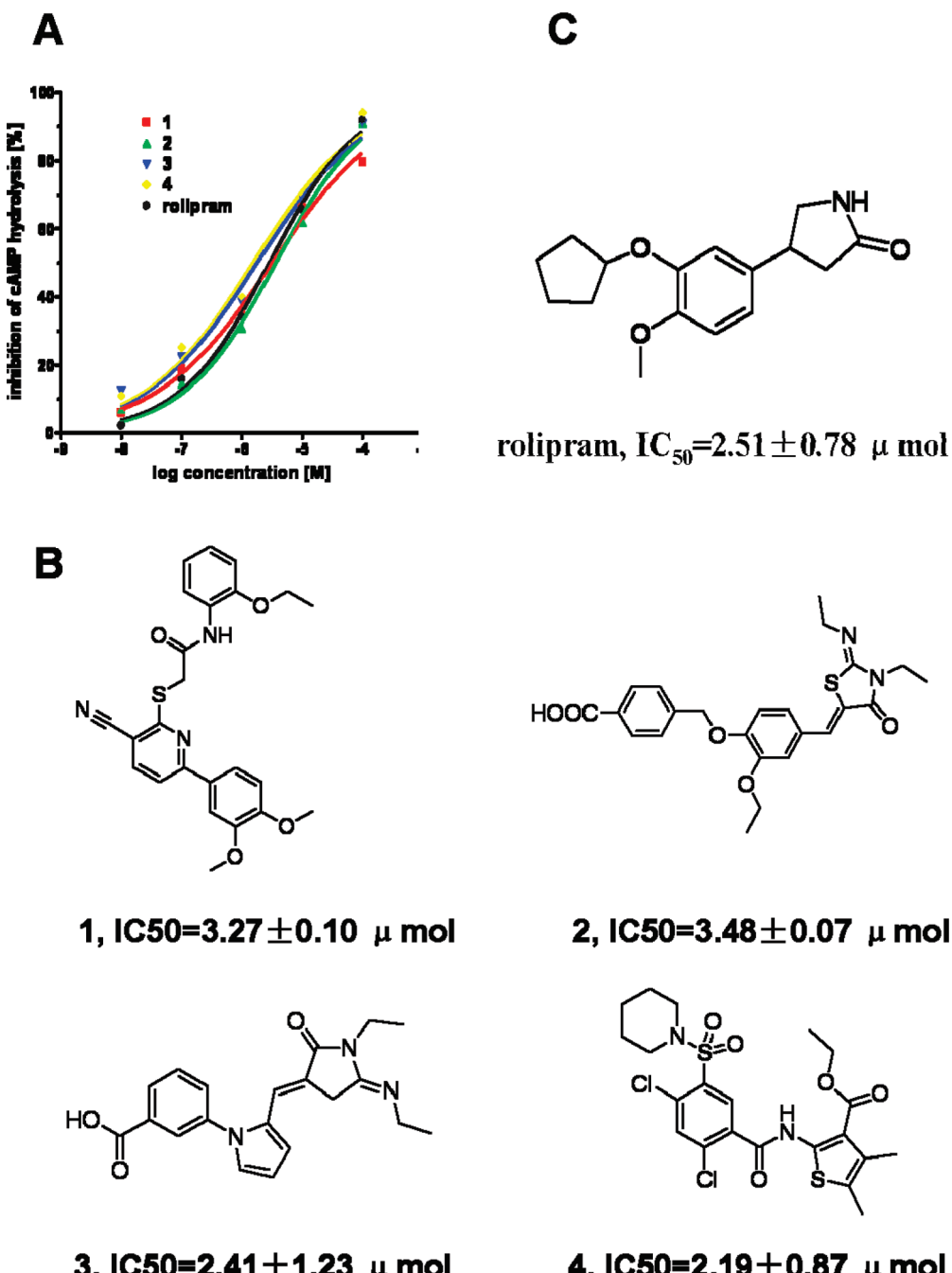


Figure 4. (A) Inhibition of PDE4 activity isolated from rat kidneys by PDE4 inhibitors. For each compound, three independent measurements were performed. Values presented are from representative experiments. (B) The structures of the four newly discovered PDE4 inhibitors with IC₅₀ displayed. (C) The structure of the positive control rolipram.

phore features and constrained information are needed to predict accurate binding conformations. Indeed, the ligand in the crystal structure of 1Y2K deduced a pharmacophore model with seven features (Figure 6B), and the conformation predicted by the pharmacophore model is exactly the same as that in the crystal structure, with a rmsd of only 0.19 Å.

Comparatively, the performance of docking program varies with different systems. For example, the ligands in 1Y2C and 1Y2H are almost the same (Figure 6C and D), but the rmsd values between the determined and the docked conformations by Glide are 0.282 Å (1Y2C, Figure 6C) and 7.303 Å (1Y2H, Figure 6D, colored cyan), respectively, have very different performances in reproducing the binding conformation. Interestingly, if a constraint of the hydrogen

bond between the inhibitor and the residue Gln443 of PDE4 is applied, the docking rmsd is 2.88 Å (Figure 6D, colored red). Another example is 1XOM, a constraint of the hydrogen bond with residue Gln369 could change the rmsd from 6.15 to 1.47 Å (Figure 6E). Therefore, constraint docking might be an ideal algorithm for reproducing better binding conformation via the docking approach.

The Hydrogen Bond with Q369/Q443 is a Common Binding Feature of the Four New Inhibitors. It is noticed that the predicted conformations of the four inhibitors by pharmacophore and docking methods are different from each other. Figure 6F is the predicted conformations of **1** by the Glide and pharmacophore methods. Both conformations have a clear hydrogen bond between the ligand and the residue

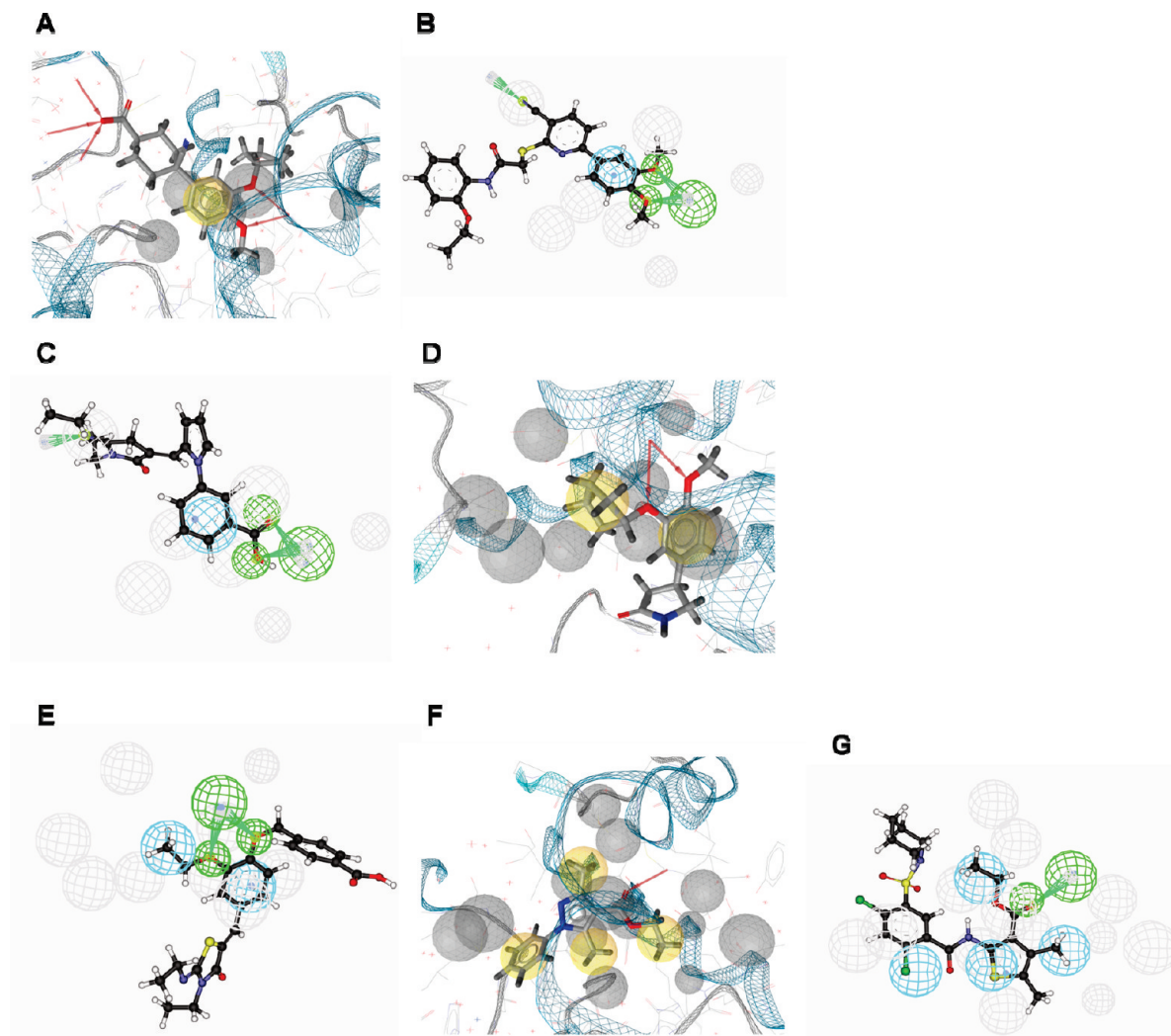


Figure 5. The mapping graphs of the active compounds to the pharmacophore models. The pharmacophore model of 1XOM-1 (A) and the mapping graphs of the inhibitor 1 (B) and 3 (C); the pharmacophore model of 1RO6-1 (D) and the mapping graph of 2 (E); the pharmacophore model of 1Y2C (F) and the mapping graphs of 4 (G).

Table 2. The RMSDs between the X-ray Determined and the Predicted Conformations of the Ligands by Catalyst, GOLD, and Glide

PDB code	catalyst	GOLD	Glide
1RO6	0.596	1.760	0.768
1TBB	1.797	0.517	1.561
1XLX	0.985	2.748	3.745
1XLZ	2.314	2.340	1.856
1XM4	1.254	1.452	0.319
1XM6	0.312	0.827	2.204
1XMU	0.312	1.645	0.645
1XOM	1.121	2.120	6.152
1XON	0.293	2.360	0.404
1XOQ	0.232	1.361	0.378
1XOR	0.470	3.965	0.743
1Y2C	0.224	0.981	0.282
1Y2E	0.465	0.884	0.513
1Y2H	0.359	1.764	7.303
1Y2J	0.653	1.703	2.928
1Y2K	0.186	3.971	3.346
2FM0	1.893	2.090	4.463
2FM5	1.446	2.253	2.187
average	0.828	1.930	2.211

Gln369, and a similar conformation of the benzene of the ligand. However, to form a hydrogen bond between the cyano

nitrogen atom of 1 and the water molecule, the pharmacophore model puts its phenyl group deep in the pocket and leads to a clash with the residues around His164. In contrast, Glide predicted a more proper conformation (Figure 6F). However, if we carefully check the conformation, we would find that the conflict could be removed by turning over the ligand, which still keeps the key interaction features. One important reason of the conflict is that the pharmacophore model omitted the residues, which do not interact with the cocrystallized ligands. Since the docking program by Glide could take into account all the residues in the binding site, it produced a proper conformation but missed the hydrogen bond with residue Glu230 (Figure 6F).

All the cocrystallized ligands in PDE4B have hydrogen bonding with Gln443 (Figure 7A), impressively, the binding conformations of the identified inhibitor 2 predicted by the pharmacophore models also displayed the hydrogen bond with Gln443 (colored cyan in Figure 7B). However, neither Glide nor GOLD did. A similar conclusion could be drawn for PDE4D. All the cocrystallized ligands interact with Gln369 by hydrogen bonds, and some of them interact with Asp318 (Figure 7C); both our pharmacophore and Glide predicted conformations of 1 maintained this hydrogen bond,

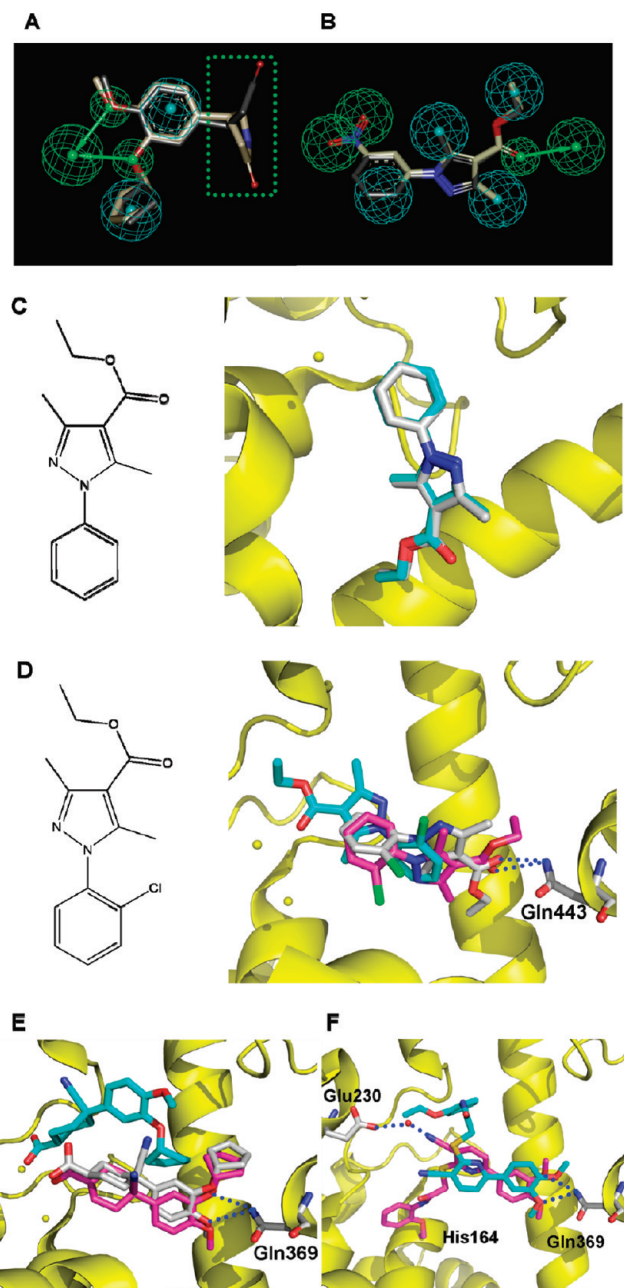


Figure 6. The comparison of the predicted and X-ray determined conformations. (A) The pharmacophore of 1TBB and the binding conformation of the ligand predicted by pharmacophore method (colored black). The original conformation of the ligand in PDB is colored gray. The excluded volumes of the pharmacophore were omitted for clarity. The green arrow and sphere represent a hydrogen-bond acceptor, and the cyan sphere represents a hydrophobic group. (B) The pharmacophore of 1Y2K and the predicted conformation by pharmacophore method. The color scheme is the same as Figure 2A. (C) The ligand in crystal structure 1Y2C (left) and the conformation predicted by Glide (right). The experimentally determined conformation is colored white, and the predicted conformation is colored cyan. (D) The ligand in crystal structure 1Y2H (left) and the conformations predicted by Glide (right). The experimentally determined conformation is colored white; the conformation predicted by Glide without any constraint is colored cyan; the conformation predicted with constraint of a hydrogen bond is colored red. The dashed blue line represents the hydrogen bond formed between ligand and residue. (E) The conformation of the ligand in 1XOM predicted by Glide. The color scheme is the same as that in Figure 2D. (F) The binding conformation of the inhibitor **1** predicted by the pharmacophore method (red) and Glide (cyan). The red sphere represents a water molecule which mediates hydrogen bond between the inhibitor and Glu230.

but GOLD did not (Figure 7D). The conformations of **3** and **4** predicted by the pharmacophore method showed this hydrogen bond, but Glide and GOLD did not (Figures 7E and F). All of the predicted binding conformations of the four actives reflected that the pharmacophore models are more reasonable than docking in reproducing binding conformation of active compounds.

Pharmacophore Search is More Powerful than Ligand Similarity Based Search. Similarity search for existing ligands is another way to find new actives in a chemical database. To make a comparison, the similarity search was performed with the tested database on the platform of the software DS. Figure 8 displays the recovery rates of the similarity search in the decoy database based on the ligands in the crystal structures, viz., 1XM6, 1XLZ, 1XMU, 1Y2J, 1Y2H, 1Y2C, 2FM0, 2FM5, 1XOM, 1XOQ, 1TBB, 1Y2E, 1XOR, 1Y2K, and 1XON. The highest recovery rate, 25.8%, in the top 5% of the ranked databases is from 2FM0 and 2FM5 (Figure 8), which is significantly lower than that of the complex structure-based pharmacophore method (47.0%, Figure 1C). Impressively, the hit rates from the two different approaches do not match each other. For example, the pharmacophore generated from 1XOM can make a recovery rate as high as 47.0%, but the similarity search based on the ligand from 1XOM only makes a recovery rate of 16.7%. The good performance of pharmacophore might be attributed to pharmacophore features for ligand binding, but the similarity search just looks for a similar group to the existing ligand, including those important and unimportant for ligand binding. This difference makes the pharmacophore method superior to similarity search.

For further comparing the similarity of the newly discovered four inhibitors to the existing ligands in PDB structures, the Tanimoto coefficients^{34,35} of the four inhibitors to the corresponding ligands were computed, which are 0.355, 0.276, 0.206, and 0.448, respectively, demonstrating a low similarity among them. If these values were used as a baseline in the similarity search against the database SPECS, they would be 15 907, 135 635, 152 047, and 10 205 compounds retrieved, much more than the corresponding pharmacophore method retrieved, while the hit numbers by the pharmacophore method are 807, 228, 9027, and 761, with the fit values of the four actives to their corresponding pharmacophore models as a baseline. This result reflected that a ligand similarity based search is much less efficient in identifying hit compounds in comparison with our approach.

Ligand–Receptor Complex-Based Pharmacophore has Better Performance than Ligand-Based Pharmacophore. To explore the advantage of the complex structure-based pharmacophore, the performance of the pharmacophore models based only on the ligands was also carried out. The 15 actives in the 18 crystal structures were extracted and produced a pharmacophore model with HipHop method in Catalyst (Figure 9). HipHop could derive a pharmacophore based on features that are common to active molecules. The generated hypothesis consists of one hydrogen-bond acceptor and three hydrophobic groups. The tested database was screened with this pharmacophore model, resulting in a recovery rate of 21.2%, not as good as the performance of structure-based pharmacophore method. In addition, the SPECS database was screened with this pharmacophore

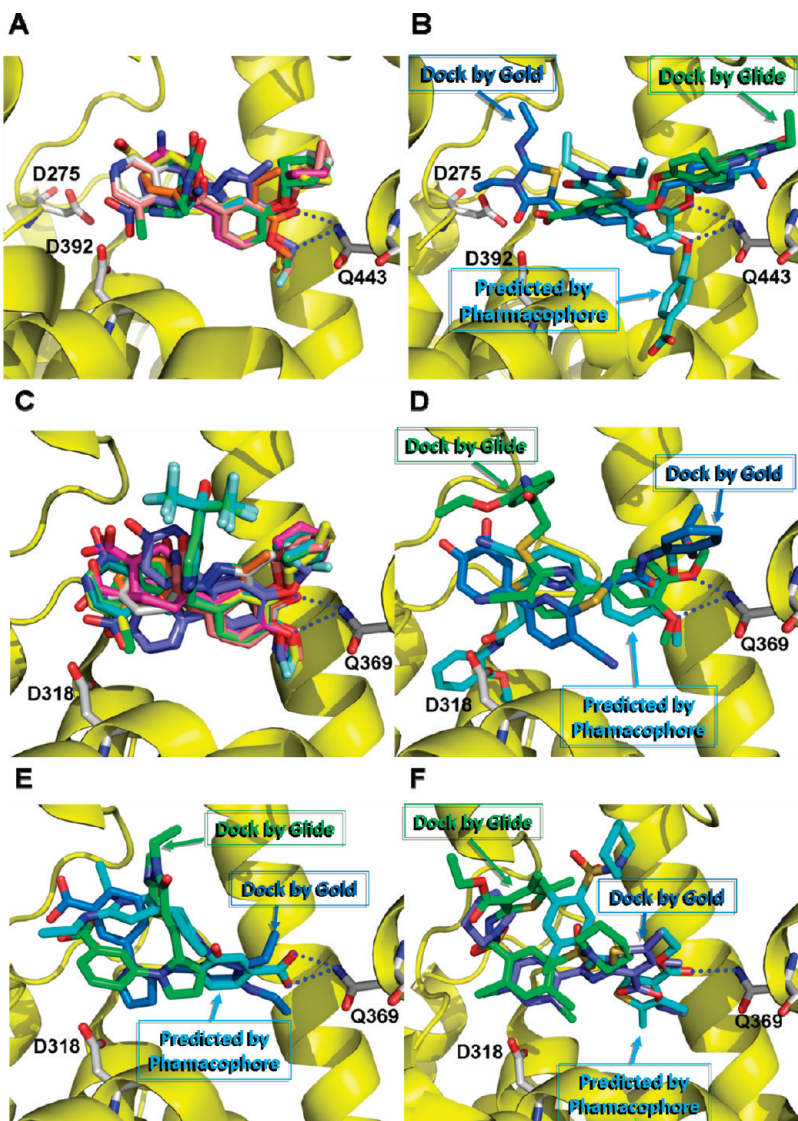


Figure 7. (A) The crystal structure of PDE4B and its cocrystallized ligands. The important residues which are involved in the interaction with the ligands are marked and shown in stick mode. (B) The conformation of **2** predicted by pharmacophore method (cyan), Glide (green), and GOLD (blue). (C) The crystal structure of PDE4D and its cocrystallized ligands. The important residues were also marked and shown in stick mode. The predicted conformations of compound **1** (D), **3** (E), and **4** (F) by pharmacophore method (cyan), Glide (green), and GOLD (blue) are displayed.

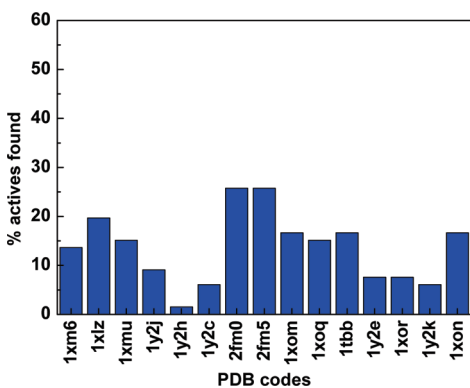


Figure 8. The recovery rate of a similarity search based on the cocrystallized ligands in crystal structures.

model, but inhibitor **1** was not successfully identified. Inhibitors **2**, **3**, and **4** could be retrieved by this pharmacophore model, but were ranked 8468, 6410, and 5564 with fit values of 3.17, 3.23, and 3.26, respectively. In contrast,

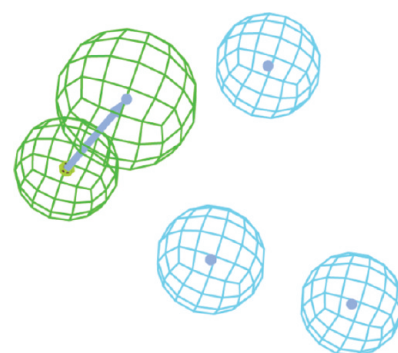


Figure 9. The pharmacophore model based on the ligands in crystal structures. The green sphere represents a hydrogen-bond acceptor and blue sphere represents a hydrophobic group.

the complex structure-based pharmacophore method yielded a rank of 228, 9027, and 761 for the three inhibitors with fit values of 3.92, 3.25, and 3.74, respectively. All these results demonstrated that the complex structure-based pharmacoph-

ore method has better performance in virtual screening. This is probably because the complex structure-based pharmacophore is based on the actual interaction reflected in the crystal structure, while that based only on ligands is not.

High Structural Diversity of the Hits by Complex Structure-Based Pharmacophore Screening. Structural diversity is an important index for the quality of the hits by an *in silico* approach. Accordingly, we compared the structural diversity of the hits retrieved from the SPECS database by three methods, viz., complex structure-based pharmacophore, ligand-based pharmacophore, and simple 2D similarity search approaches. The diversity is measured by number assemblies, which is defined as the total number of assemblies divided by the number of molecules and is calculated by DS. The calculated number assemblies are 0.297, 0.279 and 0.283, respectively, implying that the hits from the complex structure-based pharmacophore screening have the most diversity in chemical structures.

CONCLUSION

In this study, multiple pharmacophore models were derived from different ligand–receptor crystal structures and were employed to screen the database SPECS for the discovery of PDE4 inhibitors. After cross-validation by docking programs, four inhibitors with an IC_{50} less than 10 μM were discovered. It is found that even for the same target, the hits retrieved by different pharmacophore models are different. In addition, the four potent inhibitors were identified by three different pharmacophore models. Systematic comparisons revealed that a ligand–receptor complex structure-based pharmacophore has advantages in efficiently identifying potent hits with great structural diversity over both a ligand-based pharmacophore and a similarity search. This result demonstrated that multiple pharmacophore models for the same target reflect different binding modes and should be used in the virtual screening. In the hit list from this study, 7.5% of the compounds with remarkable structural diversity were identified as effective PDE4 inhibitors as active as well-known positive control rolipram, demonstrating that multiple pharmacophore models combined with a docking approach is an efficient and more reliable way and should be employed, if available, for thoroughly discovering potential hits from a chemical database.

ACKNOWLEDGMENT

The authors gratefully acknowledge financial support the 863 Program (Grant no. 2007AA02Z145 and 2006AA02Z336), the International Collaboration Project (Grant no. 2007DFB30370), ACS Innovation Program (Grant no. KSCX2-YW-R-18) and National Science and Technology Major Project (2009ZX09301-001).

Supporting Information Available: Twenty-two refined pharmacophore models for PDE4B and PDE4D in the data set. This material is available free of charge via the Internet at <http://pubs.acs.org>.

REFERENCES AND NOTES

- Stahl, M.; Guba, W.; Kansy, M. Integrating molecular design resources within modern drug discovery research: the Roche experience. *Drug Discovery Today* **2006**, *11* (7–8), 326–333.
- Kurogi, Y.; Guner, O. F. Pharmacophore modeling and three-dimensional database searching for drug design using catalyst. *Curr. Med. Chem.* **2001**, *8* (9), 1035–1055.
- Guner, O.; Clement, O.; Kurogi, Y. Pharmacophore modeling and three dimensional database searching for drug design using catalyst: recent advances. *Curr. Med. Chem.* **2004**, *11* (22), 2991–3005.
- Steindl, T. M.; Schuster, D.; Wolber, G.; Laggner, C.; Langer, T. High-throughput structure-based pharmacophore modelling as a basis for successful parallel virtual screening. *J. Comput.-Aided Mol. Des* **2006**, *20* (12), 703–715.
- Wolber, G.; Langer, T. LigandScout: 3-D pharmacophores derived from protein-bound ligands and their use as virtual screening filters. *J. Chem. Inf. Model.* **2005**, *45* (1), 160–169.
- Langer, T.; Krobat, E. M. Chemical feature-based pharmacophores and virtual library screening for discovery of new leads. *Curr. Opin. Drug Discovery Devel.* **2003**, *6* (3), 370–376.
- Krobat, E. M.; Fruhwirth, K. H.; Langer, T. Pharmacophore identification, *in silico* screening, and virtual library design for inhibitors of the human factor Xa. *J. Chem. Inf. Model.* **2005**, *45* (1), 146–159.
- Jeon, Y. H.; Heo, Y. S.; Kim, C. M.; Hyun, Y. L.; Lee, T. G.; Ro, S.; Cho, J. M. Phosphodiesterase: overview of protein structures, potential therapeutic applications and recent progress in drug development. *Cell. Mol. Life Sci.* **2005**, *62* (11), 1198–1220.
- Xu, R. X.; Hassell, A. M.; Vanderwall, D.; Lambert, M. H.; Holmes, W. D.; Luther, M. A.; Rocque, W. J.; Milburn, M. V.; Zhao, Y.; Ke, H.; Nolte, R. T. Atomic structure of PDE4: insights into phosphodiesterase mechanism and specificity. *Science* **2000**, *288* (5472), 1822–1825.
- Conti, M.; Jin, S. L.; Monaco, L.; Repaske, D. R.; Swinnen, J. V. Hormonal regulation of cyclic nucleotide phosphodiesterases. *Endocr. Rev.* **1991**, *12* (3), 218–234.
- Teixeira, M. M.; Gristwood, R. W.; Cooper, N.; Hellewell, P. G. Phosphodiesterase (PDE)4 inhibitors: anti-inflammatory drugs of the future? *Trends Pharmacol. Sci.* **1997**, *18* (5), 164–171.
- Spina, D. PDE4 inhibitors: current status. *Br. J. Pharmacol.* **2008**, *155* (3), 308–315.
- Rabe, K. F.; Bateman, E. D.; O'Donnell, D.; Witte, S.; Bredenbroker, D.; Bethke, T. D. Roflumilast—an oral anti-inflammatory treatment for chronic obstructive pulmonary disease: a randomised controlled trial. *Lancet* **2005**, *366* (9485), 563–571.
- Calverley, P. M.; Sanchez-Toril, F.; McIvor, A.; Teichmann, P.; Bredenbroker, D.; Fabbri, L. M. Effect of 1-year treatment with roflumilast in severe chronic obstructive pulmonary disease. *Am. J. Respir. Crit. Care Med.* **2007**, *176* (2), 154–161.
- Rennard, S. I.; Schachter, N.; Strek, M.; Rickard, K.; Amit, O. Cilomilast for COPD: results of a 6-month, placebo-controlled study of a potent, selective inhibitor of phosphodiesterase 4. *Chest* **2006**, *129* (1), 56–66.
- Krier, M.; Araujo-Junior, J. X.; Schmitt, M.; Duranton, J.; Justiano-Basarán, H.; Lugnier, C.; Bourguignon, J. J.; Rognan, D. Design of small-sized libraries by combinatorial assembly of linkers and functional groups to a given scaffold: application to the structure-based optimization of a phosphodiesterase 4 inhibitor. *J. Med. Chem.* **2005**, *48* (11), 3816–3822.
- Rizzi, A.; Fioni, A. Virtual screening using PLS discriminant analysis and ROC curve approach: an application study on PDE4 inhibitors. *J. Chem. Inf. Model.* **2008**, *48* (8), 1686–1692.
- Ducrot, P.; Andrianjara, C. R.; Wrigglesworth, R. CoMFA and CoMSIA 3D-quantitative structure-activity relationship model on benzodiazepine derivatives, inhibitors of phosphodiesterase IV. *J. Comput.-Aided Mol. Des* **2001**, *15* (9), 767–785.
- Jones, G.; Willett, P.; Glen, R. C. Molecular recognition of receptor sites using a genetic algorithm with a description of desolvation. *J. Mol. Biol.* **1995**, *245* (1), 43–53.
- Jones, G.; Willett, P.; Glen, R. C.; Leach, A. R.; Taylor, R. Development and validation of a genetic algorithm for flexible docking. *J. Mol. Biol.* **1997**, *267* (3), 727–748.
- Verdonk, M. L.; Cole, J. C.; Hartshorn, M. J.; Murray, C. W.; Taylor, R. D. Improved protein-ligand docking using GOLD. *Proteins* **2003**, *52* (4), 609–623.
- Friesner, R. A.; Banks, J. L.; Murphy, R. B.; Halgren, T. A.; Klicic, J. J.; Mainz, D. T.; Repasky, M. P.; Knoll, E. H.; Shelley, M.; Perry, J. K.; Shaw, D. E.; Francis, P.; Shenkin, P. S. Glide: a new approach for rapid, accurate docking and scoring. 1. Method and assessment of docking accuracy. *J. Med. Chem.* **2004**, *47* (7), 1739–1749.
- Friesner, R. A.; Murphy, R. B.; Repasky, M. P.; Frye, L. L.; Greenwood, J. R.; Halgren, T. A.; Sanschagrin, P. C.; Mainz, D. T. Extra precision glide: docking and scoring incorporating a model of hydrophobic enclosure for protein-ligand complexes. *J. Med. Chem.* **2006**, *49* (21), 6177–6196.
- Berman, H. M.; Westbrook, J.; Feng, Z.; Gilliland, G.; Bhat, T. N.; Weisig, H.; Shindyalov, I. N.; Bourne, P. E. The Protein Data Bank. *Nucleic Acids Res.* **2000**, *28* (1), 235–242.

- (25) Palmer, A.; Cabre, F.; Pascual, J.; Campos, J.; Trujillo, M. A.; Entrena, A.; Gallo, M. A.; Garcia, L.; Mauleon, D.; Espinosa, A. Identification of novel cyclooxygenase-2 selective inhibitors using pharmacophore models. *J. Med. Chem.* **2002**, *45* (7), 1402–1411.
- (26) Norinder, U. Refinement of Catalyst hypotheses using simplex optimization. *J. Comput.-Aided Mol. Des.* **2000**, *14* (6), 545–557.
- (27) Greenidge, P. A.; Carlsson, B.; Bladh, L. G.; Gillner, M. Pharmacophores incorporating numerous excluded volumes defined by X-ray crystallographic structure in three-dimensional database searching: application to the thyroid hormone receptor. *J. Med. Chem.* **1998**, *41* (14), 2503–2512.
- (28) Huang, N.; Shoichet, B. K.; Irwin, J. J. Benchmarking sets for molecular docking. *J. Med. Chem.* **2006**, *49* (23), 6789–6801.
- (29) Pages, L.; Gavalda, A.; Lehner, M. D. PDE4 inhibitors: a review of current developments (2005 - 2009). *Expert Opin. Ther. Pat.* **2009**, *19* (11), 1501–1519.
- (30) Xu, R. X.; Rocque, W. J.; Lambert, M. H.; Vanderwall, D. E.; Luther, M. A.; Nolte, R. T. Crystal structures of the catalytic domain of phosphodiesterase 4B complexed with AMP, 8-Br-AMP, and rolipram. *J. Mol. Biol.* **2004**, *337* (2), 355–365.
- (31) Huai, Q.; Sun, Y.; Wang, H.; Macdonald, D.; Aspiotis, R.; Robinson, H.; Huang, Z.; Ke, H. Enantiomer discrimination illustrated by the high resolution crystal structures of type 4 phosphodiesterase. *J. Med. Chem.* **2006**, *49* (6), 1867–1873.
- (32) Shin, H. J.; Kim, H. J.; Kwak, J. H.; Chun, H. O.; Kim, J. H.; Park, H.; Kim, D. H.; Lee, Y. S. A prenylated flavonol, sophoflavesceol: a potent and selective inhibitor of cGMP phosphodiesterase 5. *Bioorg. Med. Chem. Lett.* **2002**, *12* (17), 2313–2316.
- (33) Card, G. L.; England, B. P.; Suzuki, Y.; Fong, D.; Powell, B.; Lee, B.; Luu, C.; Tabrizizad, M.; Gillette, S.; Ibrahim, P. N.; Artis, D. R.; Bollag, G.; Milburn, M. V.; Kim, S. H.; Schlessinger, J.; Zhang, K. Y. Structural basis for the activity of drugs that inhibit phosphodiesterases. *Structure* **2004**, *12* (12), 2233–2247.
- (34) Flower, D. R. On the properties of bit string-based measures of chemical similarity. *J. Chem. Inf. Comput. Sci.* **1998**, *38*, 379–386.
- (35) Willett, P. Chemical similarity searching. *J. Chem. Inf. Comput. Sci.* **1998**, *38*, 983–996.

CI9004173